J Mater Sci (2007) 42:6139–6147
DOI 10.1007/s10853-006-0982-y

# Magnetically actuable polymer nanocomposites for bioengineering applications

**Julia J. Mack · Brian N. Cox · Min Lee · James C. Y. Dunn · Benjamin W. Wu**

Received: 14 March 2006 / Accepted: 21 September 2006 / Published online: 17 April 2007


**Abstract** Methods are presented for creating biocompatible composites with magnetic functionality by incorporating magnetic nanoparticles in a biodegradable polymer matrix. A wide range of volume fractions for magnetic particle loading and therefore magnetization density are achievable. The nanoscale of the particles aids in achieving dispersion, so that variations in physical and chemical properties occur on scales much less than that of cells. Sufficient magnetization is achieved to enable actuation of the material, i.e., the generation of strains of biologically significant magnitudes using remotely applied magnetic fields. The magnitude of the actuation is demonstrated to enable fluid pumping and create local strains in cell aggregates that should be sufficient to stimulate cell growth and differentiation. The composite materials can be formed into random-pore scaffold materials with controlled porosity, pore shape, and pore connectivity. They can also be shaped by pressing, rolling, or drawing and joined by thermoplastic welding, so that ordered three-dimensional scaffold structures and various shell structures, such as tubes and toroids, can be fabricated. When the composite sheets are formed into tubes, the application of a moving magnetic field induces simulated peristalsis. When intestinal cells were seeded on the composite sheets, cells remained viable and grew rapidly in vitro.

J. J. Mack (✉) · B. N. Cox
Teledyne Scientific Company, 1049 Camino Dos Rios, Thousand Oaks, CA 91360, USA
e-mail: jmack@teledyne.com

M. Lee · J. C. Y. Dunn · B. W. Wu
Department of Bioengineering, University of California, Los Angeles, 420 Westwood Plaza, Room 7523 Boelter Hall, P.O. Box 951600, Los Angeles, CA 90095-1600, USA

J. C. Y. Dunn
Department of Surgery, University of California, Los Angeles, 10833 Le Conte Avenue, Box 709818, Los Angeles, CA 90095, USA

## Introduction

A primary challenge in tissue engineering is achieving structure and shape in an aggregate of cells. Growing cells either in vitro or in vivo into the correctly organized, three-dimensional structures that are found in organs or tissue is made difficult by the cells' inability to grow independently, in a self-supporting manner, into targeted orientations and shapes. Therefore the art of tissue engineering proceeds by the seeding and attachment of cells onto a biocompatible and biodegradable scaffold, which can to some extent guide the development of the correct cellular structure.

The choice of scaffold is critical to enabling the cells to produce tissues and organs of the desired shape and size. Scaffold characteristics that have become recognized as critical to successful tissue engineering include (1) using a material of controlled biodegradability so that tissue will eventually replace the scaffold, (2) having an open three-dimensional structure to favor tissue integration and vascularization, (3) achieving appropriate surface chemistry to favor cell attachment, differentiation, and proliferation, (4) providing adequate mechanical properties for implantation and handling, and (5) allowing for the ingress of cells and nutrients [1, 2]. Scaffolds with most or all of these characteristics are now available. However, further control of cell growth and differentiation could possibly be achieved by adding two mechanical functionalities to the scaffold,

the ability to pump fluids and the ability to impose mechanical strains on the cells. Both of these functions could be effected in vivo in a non-intrusive manner if scaffolds could be developed that can be actuated by the remote application of magnetic fields. In particular, methods are sought to cause scaffold motion without the need for intrusive electrical leads or implanted mechanical strain actuation devices.

Presented in this article are specific methods to fabricate magnetically modified biocompatible polymers, which can be actuated by remotely applied magnetic fields. The magnitude of the actuation is shown to be biologically useful by simple tests in known magnetic fields and magnetic field gradients. A number of methods of processing the functionalized polymers into scaffolds and other structures are demonstrated, suggesting wide applicability in tissue engineering and other bioengineering fields.

The materials needed to achieve magnetically functionalized scaffolds are sought among those that are known to be biocompatible and biodegradable. A popular class of synthetic resorbable polymers is aliphatic polyesters such as polyglycolic acid (PGA) and polylactic acid (PLA). Copolymers of PGA and PLA, poly(lactide-co-glycolide) (PLGA) are amorphous and degrade by hydrolysis. The degradation products are present in the human body and removed by natural metabolic pathways. The degradation is fast and can be controlled by molecular weight, crystallinity, and ratio of lactide to glycolide [3]. PLGA is also an attractive scaffold material because of its thermoplastic properties and flexibility, which allow easy processing into a variety of configurations. Schemes for controlling the final shape of an organ or regenerated tissue via scaffold geometry could be realized.

The selection of the magnetic additive is guided partly by biocompatibility and biodegradability, but also by characteristics that will determine the magnetic functionality of the composite. For example, magnetic nanoparticles with a high aspect ratio create a shape anisotropy effect, which could be exploited to generate force moments in an applied field. Spherical magnetic particles at the nanoscale tend to be superparamagnetic and therefore give rise to distributed body forces in an applied field gradient. Further considerations in choosing magnetic materials refer to the ability to create a dense dispersion of magnetic material and to control particle clustering.

This article presents preliminary data acquired for one particular novel material system, with implications of the possibility of fabricating many more in the class. Various prototype scaffold structures are demonstrated and preliminary tests of biocompatibility and the viability of cells seeded on the materials are reported.

## Materials and methods

### Materials

Poly(D,L-lactide-co-glycolide) (PLGA) with a lactide to glycolide molar ratio of 65:35 (intrinsic viscosity 0.53 dL/g) was purchased from Lakeshore Biomaterials Inc. (Birmingham, Alabama). Nanorods of maghemite ($\gamma$-$Fe_2O_3$) were obtained from Titan Kogyo, Japan (AUVICO ATG-2600). The $\gamma$-$Fe_2O_3$ nanorods were estimated to be approximately 60 nm in diameter by 300 nm in length via scanning electron microscopy (SEM) (Fig. 1). Anhydrous chloroform was purchased from Sigma Aldrich (St. Louis, Missouri) and used as received.

### Composite solutions

Dispersions of $\gamma$-$Fe_2O_3$ in PLGA were prepared with concentrations ranging from 10 to 30 wt.% $\gamma$-$Fe_2O_3$ (based on PLGA). A typical composite solution was prepared by weighing 2.0 g of PLGA pellets in a glass vial and adding 0.4 g $\gamma$-$Fe_2O_3$ powder, to which 10 mL of chloroform is added as solvent. The solution was agitated on an orbital shaker for approximately 2 h or until the PLGA was completely dissolved. To aid in dispersion of the $\gamma$-$Fe_2O_3$ nanorods, the composite solution was placed in an ultrasonic bath for ~5 min prior to casting.

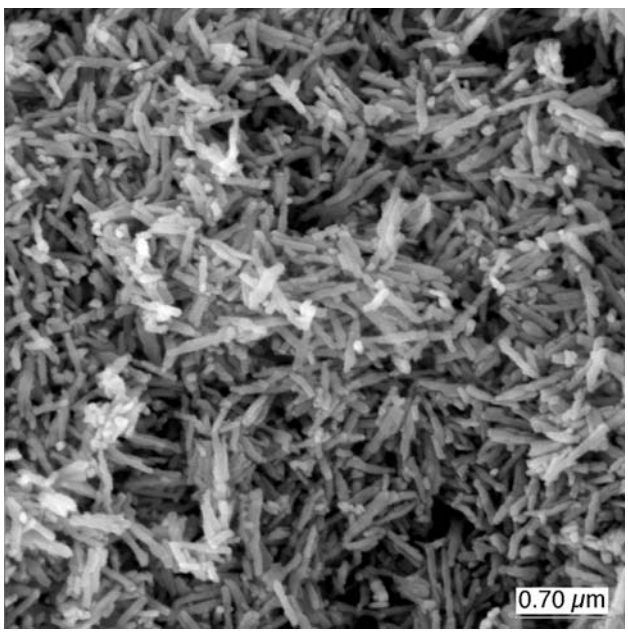


**Fig. 1** SEM image of $\gamma$-$Fe_2O_3$ nanorods

### Casting and curing of composite sheets

Poly(lactide-co-glycolide), like most polymers, can be cast into films or sheets. The size of the casting mold as well as the viscosity of the polymer solution will help determine the film thickness. In general, the polymer should be dissolved in a volatile solvent using a fairly high solids content. The solution should then be poured into the appropriate mold size to achieve the desired thickness after solvent evaporation. The solvent can be removed via evaporation in a hood or by vacuum. The application of some heat can speed the process, but care should be taken not to exceed the glass transition temperature.

To form sheets of $\gamma$-$Fe_2O_3$/PLGA, the composite solution was poured into a silicone mold. An appropriate amount of solution was added to form the desired sheet thickness. The $\gamma$-$Fe_2O_3$/PLGA/chloroform dispersion was allowed to cure by solvent evaporation in a hood at room temperature for 1–2 days. Once the chloroform has been completely evaporated, the composite sheet can be easily removed from the silicone mold.

The formation of thin sheets and thick films of the cast $\gamma$-$Fe_2O_3$/PLGA composite can also be aided by pressure and heat. In a double-plate heated hydraulic Carver press, for example, Teflon-coated metal plates were heated to ≤50 °C and the composite sheets were pressed into sheets of thickness 50–200 μm, depending on heating times and applied pressure. The pressure applied was typically between 500 and 3,000 psi.

### Porous scaffold formation

To form random open pore scaffolds, the $\gamma$-$Fe_2O_3$/PLGA/chloroform dispersion was mixed into a viscous paste with sugar crystals, which serve as a porogen. The paste was then packed in a Teflon mold of desired shape and size. The solvent was removed via freeze-drying (–110 °C) under dynamic vacuum (<100 mtorr). The $\gamma$-$Fe_2O_3$/PLGA/sugar composite was then soaked in water to remove the porogen.[1] The resulting porosity and interconnectivity can be controlled by the amount of sugar added and pore size can be controlled by the sugar crystal size.

### Physical characterization

Specimens for SEM were prepared by affixing with carbon tape and sputtering with a thin gold coating. Images were obtained using a Philips FEI XL30 SEM at 10 kV. Magnetic actuation was tested by measuring the force exerted on solid (cast) and porous specimens of $\gamma$-$Fe_2O_3$/PLGA composite in a balance beam apparatus and measuring the deflection of a cantilever beam composed of porous $\gamma$-$Fe_2O_3$/PLGA composite.

### Seeding of scaffolds

IEC6 cells were purchased from ATCC (Manassas, Virginia). Cells were transfected with a lentivirus that expressed the green fluorescent protein (GFP). A subclone of the transfected cells was selected by limited dilution and was expanded in culture medium containing Dulbecco's modified Eagle's medium with low glucose, 5% fetal bovine serum, 10 μg/mL insulin, and 100 U/mL penicillin and 100 μg/mL streptomycin (Gibco, Gaithersburg, Maryland) [4]. Composite films were disinfected in 70% ethanol for 20 min and rinsed in phosphate buffered saline three times before immersion in culture medium for 1 h. Each film was seeded with a density of $1.5 \times 10^4$ cells/cm$^2$ in 24-well plates and incubated in 37 °C, 10% $CO_2$, humidified incubators.

### Cell viability testing

Growth of cells on the composite films was determined by observing GFP-labeled cells under epi-fluorescence. Images of fluorescent cells were captured in a RGB color digital camera (Optronics, Goleta, California) with a Leica DM IRB light microscope (Leica Microsystems Inc., Bannockburn, Illinois) after 1, 4, and 7 days of culture. Pristine PLGA films served as control.

## Results and discussion

### Physical and mechanical properties of $\gamma$-$Fe_2O_3$/PLGA composites

Data are reported in the following for $\gamma$-$Fe_2O_3$/PLGA composites in which the $\gamma$-$Fe_2O_3$ constituted approximately 30% by weight (6.7% by volume) of the solid composite material (exclusive of porosity). The density of PLGA is 1.3 mg/m$^3$, that of $\gamma$-$Fe_2O_3$ is 6.1 mg/m$^3$, and therefore that of the $\gamma$-$Fe_2O_3$/PLGA composite is 1.59 mg/m$^3$. Since the

[1] The particulate leaching protocol of porogen removal involves repeated rinses and replenishment of large volumes of water. We have evaluated this issue on a field emission high resolution SEM and found that using our porogen removal protocol, most of the porogens are removed after the first rinse, and all of the porogens are removed after the second rinse, but we typically rinse four times. The resultant porosity has never presented any problem to cell seeding. Additionally, we have prepared five micron thick sections of the scaffolds within 1 h of cell seeding and we have never noticed the presence of porogens. While the possibility exists that a minute, negligible fraction of nanosized porogens can remain encapsulated, we are highly confident that most of the porogens are removed given the large interconnectivity of the pores, relatively small volume fraction of the polymer and the fast dissolution rate of sugar in water.

mass ratio of the mixture used to form a porous scaffold was 0.2 g PLGA:2.8 g sugar:0.06 g $\gamma$-$Fe_2O_3$ and the density of sugar is 1.59 mg/m$^3$, the random pore scaffold material is estimated to have 92% porosity.

The modulus of the random pore scaffold material was measured by compressing a block of the material between two flat platens. An initially nonlinear regime, which is caused by imperfect initial contact between the slightly rough specimen and the platens, is followed by a linear regime (Fig. 2), whose slope gives the plane-strain modulus, $E' = E/(1 - \nu^2)$, where $E$ and $\nu$ are Young's modulus and Poisson's ratio, respectively. From a number of tests, $E' = 0.53 \pm 0.1$ MPa. This stiffness is somewhat greater than that of cells: a single cell, e.g., a red blood cell, has a representative modulus of 1,000 Pa; for a cell agglomerate with an extracellular matrix of collagen and elastin, the modulus will rise significantly from this order of magnitude, but typically not exceed 0.5 MPa for soft tissues. Therefore, provided magnetic actuation can overcome the stiffness of the scaffold itself, the forces will be large enough to generate significant strains in cells contained within the scaffold.

## Forces acting on composite sheets in magnetic fields

The application of a magnetic field to a composite of magnetic nano-particles (e.g., $\gamma$-$Fe_2O_3$) dispersed in a non-magnetic medium (e.g., PLGA) will result in body forces and moments distributed throughout the material, which arise from the interaction of the magnetic particles with the field. Assuming that particle–particle interactions are weak (an applicable condition for the particle volume fraction in the preliminary scaffolds reported here), two systems of forces are possibly significant. First, a particle bearing a magnetic moment, $\boldsymbol{\mu}$, in a magnetic field gradient, d$\boldsymbol{B}$/d$x$, will be acted on by a body force, $\boldsymbol{F}$, given by [5, 6]

$$\mathbf{F} = \boldsymbol{\mu} \cdot \frac{\mathrm{d}\mathbf{B}}{\mathrm{d}x} \tag{1}$$

This force tends to displace the material in the direction of the field gradient. It is greatest in magnitude if the moment is aligned with the field gradient. This will be the case if the particles are paramagnetic, because the magnetic moment is then solely induced by the applied field and will align with the field.

If the particles are ferromagnetic (permanent magnetization that remains when the applied field is removed), then the applied field will tend to rotate the magnetic moment of the particle into alignment. If the moment can rotate easily, then the force acting on the particle will again be given by Eq. 1. However, if the magnetic particles are acicular in shape, the phenomenon of shape anisotropy in the magnetization will favor alignment of the moment with the axis of the particles; or if crystalline anisotropy is present, the moment will tend to align with a preferred crystal axis. If either of these effects is sufficiently strong, the moment will not rotate relative to the particle, but instead the particle itself will tend to rotate under a force moment or torque, $\boldsymbol{T}$, given by

$$\mathbf{F} = \boldsymbol{\mu} \times \mathbf{B} \tag{2}$$

The torque is greatest if the moment and the field are orthogonal. Equation 2 implies a distribution of moments throughout the composite, which will tend to bend or rotate the material. This effect is of interest because it raises the possibility of additional control over the characteristics of the motion induced in a scaffold. For example, by exploiting the vector nature of Eq. 2, different rotations can be induced in different parts of the scaffold by locally ordering the magnetization in different directions.

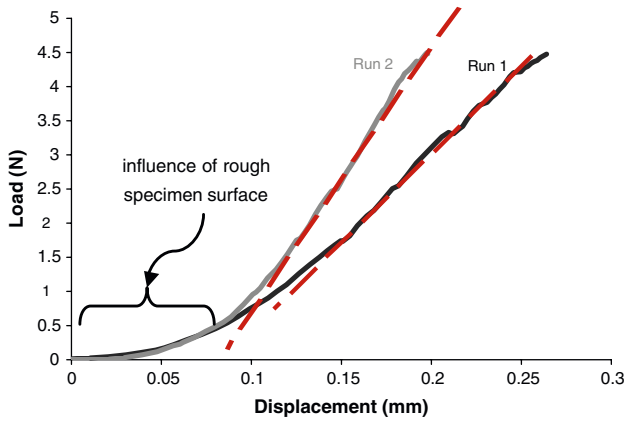


**Fig. 2** Compression test of porous scaffold material (poly(lactide-co-glycolide) (PLGA) with 30 wt.% $\gamma$-$Fe_2O_3$ in an open cell structure with porosity 91.5%)

## Magnetic properties of the $\gamma$-$Fe_2O_3$/PLGA composites

The magnetic properties of $\gamma$-$Fe_2O_3$/PLGA specimens were measured using a superconducting quantum interference device (SQUID). A typical hysteresis loop measured at room temperature is shown in Fig. 3. The saturation magnetization (magnetic moment per unit volume, $M_{solid}$) ranged from 13 to 23 emu/g (or 95,000–170,000 A/m, given a material density of 1.6 mg/m$^3$), with the variability attributed to inconstancy in the volume fraction of the magnetic particles in different specimens and variations in the clustering and orientation distribution of the particles. These factors were not perfectly controlled in the processing.

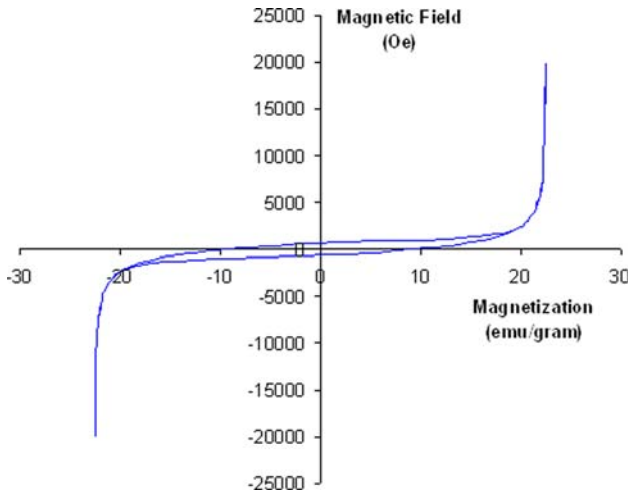


**Fig. 3** Typical magnetization vs. applied field strength data from superconducting quantum interference device (SQUID) measurements for solid $\gamma$-$Fe_2O_3$/ poly(lactide-co-glycolide) composite specimens with 30 wt.% $\gamma$-$Fe_2O_3$

The very small hysteresis and the absence of a significant coercive force in the magnetization data imply that the $\gamma$-$Fe_2O_3$ particles exist in a ferromagnetic state, with weak interactions between the moments on different particles and very little shape anisotropy effect within each particle. Thus when a magnetic field is applied, the moment in each particle rotates easily towards the direction of the applied field. Saturation magnetization is reached when the alignment is complete. In the absence of a field, the moments on different particles return to a state in which they are only weakly correlated. For a system that behaves like this, the predominant magnetic forces will be those that arise in a field gradient (Eq. 1). For a given field gradient, the force on the material will be saturated when the strength of the applied field, $\boldsymbol{H}$, exceeds approximately 2 kOe ($2 \times 10^6$ A/m) (or the magnitude of $\boldsymbol{B}$ exceeds approximately 2 kG, 0.2 T).

## Magnetic force measurements

A number of demonstrations of magnetic force effects were carried out using a small permanent magnet. The permanent magnet was a cylinder of length 3.8 cm and diameter 2.4 cm, poled so that its magnetization was parallel to its axis. The magnetic field was measured with a Gauss-meter (a small current loop on the end of a slender probe). The field is strongest as it emerges from either of the flat faces and is relatively weak along the curved sides. In the field emerging from the flat faces, a strong gradient arises in the direction of the axis of the magnet; the field falls with distance from the magnet. For the distances at which the materials were placed during the following tests, the field strength, $B$, ranged from approximately 2–4 kG and the field gradient from approximately 1–4 kG/cm (10–40 T/m). Thus the fields exceeded those required, according to the SQUID measurements, to achieve near-saturation of the magnetization.

In qualitative tests using a combination of finger touch and observation of the movement of the $\gamma$-$Fe_2O_3$/PLGA, the forces on the $\gamma$-$Fe_2O_3$/PLGA were seen always to act towards the magnet along its axis. This did not change when the initial orientation of the samples or the magnet was reversed or when different samples were substituted in the test. These observations are consistent with the measured magnetic hysteresis: the magnetization in the $\gamma$-$Fe_2O_3$/PLGA material re-aligns with the applied field; shape anisotropy is not sufficient to maintain alignment of the magnetization in a particle with its own axis.

Quantitative measurements of the magnetic forces were made using a balance beam apparatus, using a sensitive load cell to measure changes in force as the distance of the magnet from the composite material was varied (Fig. 4). Figure 5 presents force versus magnetic field gradient data for two $\gamma$-$Fe_2O_3$/PLGA composite specimens, which differed in mass as shown. The curves shown are smoothing curves through the data and are consistent with expectations; some variance from linearity is expected in the data, since the dimensions of the samples are not small compared to the field gradient and therefore different parts of the specimen will experience somewhat different force per unit volume.

The datum indicated by the open circle in Fig. 5 is approximately representative of all the data in the ratio of force to field gradient. For this datum, the magnetic moment per unit volume, $M_{solid}$, in the $\gamma$-$Fe_2O_3$/PLGA material is deduced to be approximately 13 emu/g (95,000 A/m). This is consistent with the range of saturation magnetization values measured in the SQUID tests.

## Actuable structures formed from thin sheets

The ability to form thin sheets enables a variety of compliant three-dimensional structures to be formed. Cast $\gamma$-$Fe_2O_3$/PLGA composite sheets can be thinned by hot-pressing between Teflon film at temperatures below 50 °C.

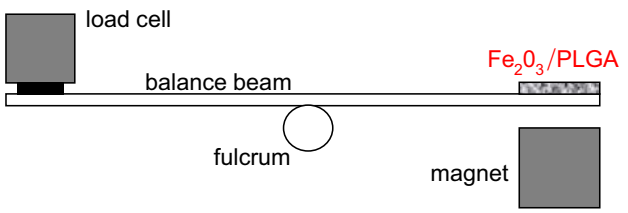


**Fig. 4** Balance beam apparatus for magnetic force measurements

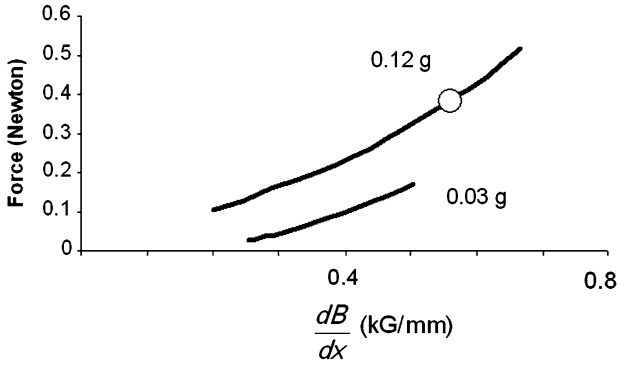


**Fig. 5** Force vs. magnetic field measurements for 30 wt.% (6.67 vol.%) $\gamma$-$Fe_2O_3$/ poly(lactide-co-glycolide) composite specimens

By varying the pressure applied, the sheet thickness can be successfully reduced to less than 75 μm, as shown in Fig. 6a. Figure 6b presents a higher resolution SEM image of the flat surface of the hot-pressed composite sheet. The $\gamma$-$Fe_2O_3$ particles are observed as agglomerates within the PLGA matrix. The agglomerated morphology, determined by fluid flow during pressing and magnetic interactions, is acceptable for magnetic actuation. Once the composite sheets are thinned, they can be joined or laminated via thermal fusion.

One simple illustrative three-dimensional structure is a tube formed by melt-forming a seam along a rolled $\gamma$-$Fe_2O_3$/PLGA composite sheet (Fig. 7). The length of the tube shown in Fig. 7 is approximately twice its diameter, but the tube is foreshortened in the figure by being viewed almost along its axis. The tube has a diameter of 22 mm, length of 44 mm and a wall thickness of 0.4 mm. The sequence of photographs shows the response of the tube to the approach of a permanent magnet; large-deflection deformation is created. The deformation is reversible. If the magnet is advanced along the length of a longer tube, a pulse of deformation is driven along its axis, creating a moving pressure gradient. The pulse of contraction provides a crude simulation of peristaltic motion. When the tube is placed in water, fluid flow can be visualized along the tube. Experiments to demonstrate fluid flow were performed on a tube with diameter of 10 mm, length of 95 mm and a wall thickness of 0.3 mm. The tube was fixed to the bottom of a water-filled container. By advancing the magnet repeatedly along the length of the tube, the moving pressure gradient was observed to drive a drop of food colorant through the tube, end to end. As well as tubes, other structures that can be formed by cutting and thermally joining thin sheets and are of interest for manipulating cells include various layered structures and ordered trusses (three-dimensional space lattices of struts and facets).

## Magnetic force acting on a porous scaffold beam

The magnetic force properties of random-pore $\gamma$-$Fe_2O_3$/PLGA scaffold material were tested by performing a simple cantilever beam experiment. The cantilever beam test was set up by taping one end of a rectangular slab of porous $\gamma$-$Fe_2O_3$/PLGA material (30 wt.% $\gamma$-$Fe_2O_3$, not counting porosity) to the surface of a glass slide with the other end left free to move. As a permanent magnet is brought up, the scaffold deflects towards the magnet (Fig. 8). To a good approximation, the deflection profile, $y(x)$, is that predicted by Euler–Bernoulli beam theory (black curve in Fig. 8b), which is given by

$$y = \frac{6qL^4}{E'h^3}\left\{\frac{1}{2}\left(\frac{x}{L}\right)^2 - \frac{1}{3}\left(\frac{x}{L}\right)^3 + \frac{1}{12}\left(\frac{x}{L}\right)^4\right\} \quad (3)$$

where $L$ and $h$ are the length and thickness of the beam (Fig. 7b) and $q$ is the magnetic force per unit area of the beam, which is assumed to act normal to the beam. With $q$ evaluated from the measured deflection and the measured field gradient at a representative separation of the deflected beam and the magnet, the magnetization per unit volume of the beam, $M_{\text{porous}}$, can be deduced. For the deflection

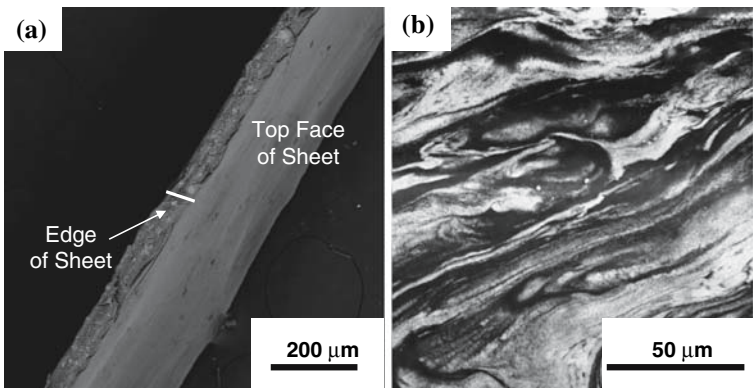


**Fig. 6** (**a**) SEM image showing the edge and flat surface of a $\gamma$-$Fe_2O_3$/poly(lactide-co-glycolide) (PLGA) composite sheet after thinning by hot-pressing between two heated metal plates. (**b**) Higher-resolution SEM image showing the flat surface of the hot-pressed $\gamma$-$Fe_2O_3$/PLGA composite sheet. The $\gamma$-$Fe_2O_3$ particles (*bright*) form agglomerates within the PLGA matrix (*dark*)

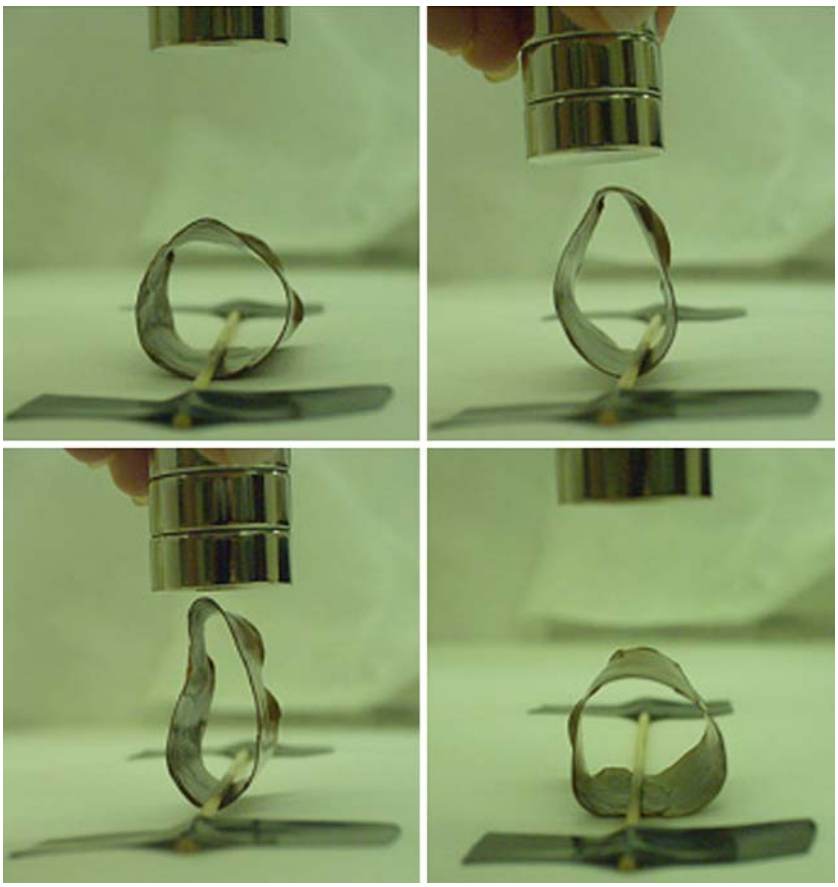

**Fig. 7** Response of 30 wt.% $\gamma$-$Fe_2O_3$/ poly(lactide-co-glycolide) composite 3-D tube with application and subsequent removal of an applied magnetic field

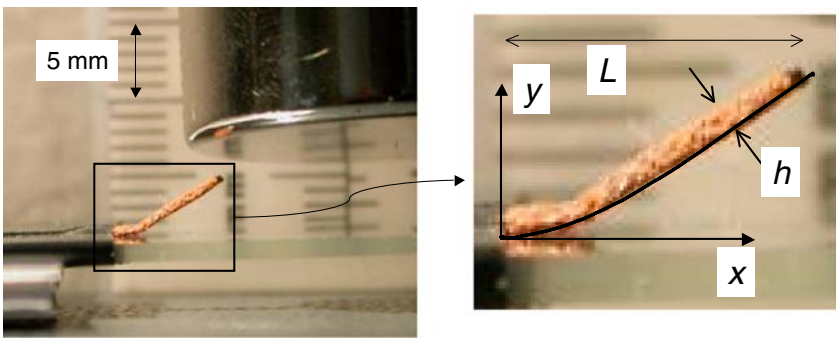


**(a)** **(b)**

**Fig. 8** Deflection of a $\gamma$-$Fe_2O_3$/ poly(lactide-co-glycolide) porous composite cantilever in a magnetic field gradient

shown in Fig. 7b, $dB/dy$ = 4.4 kG/cm (44 T/m) and $q$ = 220 N/m$^2$; and together with $E'$ = 0.50 MPa, these data lead to $M_{porous}$ = 8,500 A/m. Multiplying this value by 1/(1 – porosity) ≈ 12 yields values that are consistent with the values $M_{solid}$ measured by either the SQUID or balance beam tests for the non-porous $\gamma$-$Fe_2O_3$/PLGA composite material. Thus the magnetization of the $\gamma$-$Fe_2O_3$/PLGA material within the walls and struts of the porous scaffold is the same as that in solid $\gamma$-$Fe_2O_3$/PLGA material: the presence of porosity does not affect the magnetic ordering.

## Potential for strain actuation

The order of magnitude of strains that can be induced in various constructs of solid and porous $\gamma$-$Fe_2O_3$/PLGA material can be summarized as follows. In the cantilever of Fig. 8, the maximum strain induced arises near the built-in end. For the deflection shown in Fig. 8b, it is approximately 13% (compressive on the top of the beam and tensile on its bottom). If uniform strain is sought, then the protypical layered configuration of Fig. 9 can be used to estimate achievable strains. A layer of porous material is

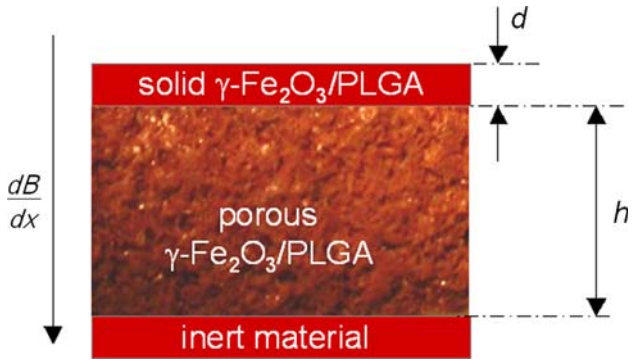


**Fig. 9** Representative configuration used to estimate order of magnitude of strains that can be actuated using present materials and fields

bounded beneath by an inert material (fixed displacement) and above by a layer of solid $\gamma$-$Fe_2O_3$/PLGA composite. If a magnetic field gradient exists in the vertical direction, a stress gradient will also arise in the material, with the largest stress (and therefore strain) in the porous material at its boundary with the inert layer. Assuming a field gradient of 5 kG/cm (50 T/m) (typical of the permanent magnet used in the tests reported above) and the magnetizations reported above for the solid and porous $\gamma$-$Fe_2O_3$/PLGA material ($M_{solid}$ = 100,000 A/m and $M_{porous}$ = 9,000 A/m), one finds the following numerical estimate for the maximum strain

$$\varepsilon_{max} \approx 10^{-3}(0.8h + 9d) \quad (h \text{ and } d \text{ in mm}) \tag{4}$$

where $h$ and $d$ are to be measured in mm and the porous material has been assigned the modulus $E'$ = 0.50 MPa. To achieve a strain of ~1% in the absence of the superficial solid $\gamma$-$Fe_2O_3$/PLGA layer ($d$ = 0), the porous layer must be ~10 mm thick. If the solid layer is present and is approximately 1 mm thick, then it alone will induce a strain throughout the porous layer of 1%.

The cantilever case shows the advantage for the maximum attainable strain magnitude of designing a structure in which members exert leveraging effects. A generalization is the truss structure or space lattice, which is an ordered assembly of struts and facets. By appropriate design, a truss can be made very compliant (more compliant for a given material density than the random pore scaffold structure), which amplifies the strains that are actuated in it by given magnetic forces.

The strains demonstrated in the preceding paragraphs are of a potentially useful range for cell stimulation and fluid pumping. Even larger strains could be created by increasing the magnetic field strength, using particulate inclusions with higher magnetization or at higher volume fractions, or using a more compliant polymer. The field strength used here (due to the permanent magnet) is approximately 5 kG (0.5 T). Fields of up to 20 kG (2 T) are regarded as safe for human use. If such a larger field is used, then, given appropriate design, the attainable field gradient should increase proportionately. Stronger forces can also be sought by using materials with higher magnetization density than $Fe_2O_3$. Rare earth magnets for which preliminary data suggest the possibility of biocompatibility include Nd–Fe–B with magnetization in the range $0.9 \times 10^6$–$1.1 \times 10^6$ A/m and Sm–Co alloys magnetization $0.7 \times 10^6$–$0.9 \times 10^6$ A/m [7]. In a 30 vol.% composite, these would dilute to ≈300,000 A/m (Nd–Fe–B) or 250,000 A/m (Sm–Co), a threefold gain over the value ~100,000 A/m for the solid $\gamma$-$Fe_2O_3$/PLGA material.

## Cell viability

Confluent cultures of GFP-labeled IEC6 cells were trypsinized and re-suspended to $3 \times 10^4$ cells/mL. The $\gamma$-$Fe_2O_3$/PLGA composite films were seeded with 1 mL of $3 \times 10^4$ cells/mL IEC6 cell suspension in the 24-well plates to evaluate the feasibility of the composite films to support cell attachment and proliferation. Cells attached to films uniformly after 1 day of culture and the cell density on the films increased with increased culture time. In order to evaluate the effect of iron oxide on the cell growth, cells were also cultured on the PLGA films not containing iron

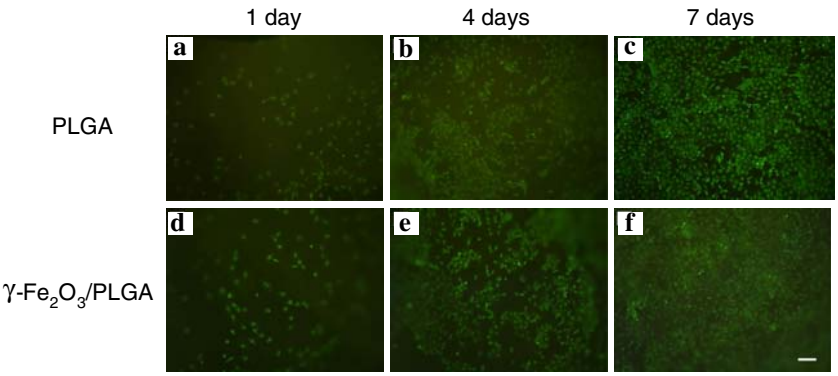


**Fig. 10** Images of cell cultures at different times, for (**a–c**) poly(lactide-co-glycolide) (PLGA) and (**d–f**) $\gamma$-$Fe_2O_3$/PLGA composite (scale bar = 100 μm)

oxide. Cell growth on the composite films was similar to the PLGA films (Fig. 10), suggesting that the $\gamma$-$Fe_2O_3$/PLGA composites have no deleterious effects for cell attachment and growth.

## Conclusion

An example has been shown of a composite system comprising magnetic particles in a biocompatible polymer in which useful levels of strain can be induced by remotely applied magnetic fields. Such an actuation method can in principle be used to actuate a scaffold in vivo, with no invasive actuating device. The strains are sufficient to stimulate cells and pump fluids to promote nutrient supply.

The exemplary material, a $\gamma$-$Fe_2O_3$/PLGA composite, shows encouraging preliminary biocompatibility results.

**Acknowledgements** The authors are very grateful to Drs. Brian Naughton and David Clarke of the University of California, Santa Barbara, for carrying out SQUID tests and to Drs. Mark Field and Jeff Cheung for instruction on magnetism.

## References

1. Hutmacher DW (2001) J Biomater Sci Polym Ed 12:107
2. Langer RS, Vacanti JP (1993) Science 160:920
3. Lemoine D, Francois C, Kedzierewicz F, Preat V, Hoffman M, Maincent P (1996) Biomaterials 17:2191
4. Lee M, Dunn JC, Wu BM (2005) Biomaterials 26(20):4281
5. Craik DJ (1995) Magnetism: principles and applications. John Wiley & Sons, New York
6. Jiles DC (1990) Introduction to magnetism and magnetic materials. Springer, New York
7. Reference and Design Manual. Dexter Magnetic Technologies Inc. http://www.dextermag.com